

SKB

**TECHNICAL
REPORT**

88-12

Near-distance seismological monitoring of the Lansjärv neotectonic fault region

Rutger Wahlström, Sven-Olof Linder, Conny Holmqvist

Seismological Department, Uppsala University, Uppsala

October 1987

NEAR-DISTANCE SEISMOLOGICAL MONITORING OF THE LANSJÄRV
NEOTECTONIC FAULT REGION

Rutger Wahlström, Sven-Olof Linder, Conny Holmqvist
Seismological Department, Uppsala University, Uppsala
October 1987

This report concerns a study which was conducted for SKB. The conclusions and viewpoints presented in the report are those of the author(s) and do not necessarily coincide with those of the client.

Information on KBS technical reports from 1977-1978 (TR 121), 1979 (TR 79-28), 1980 (TR 80-26), 1981 (TR 81-17), 1982 (TR 82-28), 1983 (TR 83-77), 1984 (TR 85-01), 1985 (TR 85-20), 1986 (TR 86-31) and 1987 (TR87-33) is available through SKB.

NEAR-DISTANCE SEISMOLOGICAL MONITORING OF THE
LANSJÄRV NEOTECTONIC FAULT REGION

Rutger Wahlström, Sven-Olof Linder and Conny Holmqvist.

Seismological Department, Uppsala University, Uppsala.

ABSTRACT

During five months in 1987, a mobile seismic network comprising digital and analog units was operated along the Lansjärv neotectonic fault segments in Swedish Lapland. More than 20 local earthquakes, at distances less than 40 km from the stations, were recorded. Nine of these have been accurately located from high-resolution digital data, using a simple velocity model derived from test explosions recorded at the stations. Two events have well restrained focal depths, 8 and 9 km, respectively. Several earthquakes are located east of the postglacial faults and in the vicinity of major faults. However, derived focal mechanisms are poorly restrained and based on data (Pg-polarities and Sg/Pg-amplitude ratios) from too few stations to allow a solid seismotectonic interpretation. Based on Sg-wave amplitude spectra, computed seismic moments range from 5×10^{10} to 1×10^{12} Nm, fault radii 40 - 100 m, average relative displacements 0.07 - 8 mm, and stress drops 0.05 - 7 MPa. A future extended network would provide more information on the detailed seismotectonic characteristics of the region.

INTRODUCTION

Svensk Kärnbränslehantering AB (Swedish Nuclear Fuel and Waste Management Co) is presently undertaking an ambitious and inter-disciplinary project on the neotectonics of Swedish Lapland, notably in the vicinity of the Lansjärv fault segments developed during or after the last deglaciation of the area some 9,000 - 10,000 years ago. The role of the Seismological Department, Uppsala University, is to operate a mobile network of analog and digital seismic stations in the vicinity of the Lansjärv faults during the periods of 1987 and 1988 when the weather conditions so permit (access to roads etc.). The first year of field work, and successive data analysis and interpretation, have been concluded, and the results are reported below.

STATIONS

The network consisted of two vertical-component analog stations, and one vertical-component and four 3-component digital stations. Signals from the single-component digital station were telemetrically transmitted to one of the 3-component units. Locations and technical data of the stations are given in Table 1, and station locations also displayed in Fig 1. Periods of operation of the different stations are shown in Fig. 2.

Several shorter intermissions at the digital stations can be ascribed to factors like bad weather (rain, wind), presence of animals, and other sources of disturbance, which have caused "false" triggers and rapid consumption of tapes. The stations F and G (Kuossakábbá + telemetry) ceased to function in late August (encoder breakdown, probably due to damp), and during the last 2-3 weeks the station B (Nitsán) had an error in the memory playback, causing loss of the initial P-wave coda (S properly recorded). The analog stations, especially D (Renberget), had reliable operations.

The time signal from OMEGA in Norway was used for most of the recording time period. It was disconnected for one week in August, during which the time signal from DCF in Germany was received.

Table 1. Locations and technical data of the stations.

Station	Code	Type	Location		Filter (Hz)	Gain (dB)
			Lat. ($^{\circ}$ N)	Lon ($^{\circ}$ E)		
Brakarberget	A	ANA	66.651	22.368	10-50	78
					(2/6-3/6)	
					5-25	78
					(3/6-5/6)	
					5-25	84
					(5/6-20/8)	
					10-25	90
					(20/8-19/10)	
Nitsån	B	DIG	66.692	22.224	0-40	GR
					(26/5-19/10)	
Kängelberget	C	DIG	66.636	22.112	0-80	48
					(22/5-26/5)	
					0-80	54
					(26/5-8/7)	
					0-80	60
					(8/7-19/10)	
Renberget	D	ANA	66.543	22.075	5-25	72
					(26/5-8/6)	
					10-50	90
					(8/6-19/10)	
Passeberget	E	DIG	66.514	21.854	0-80	60
					(1/6-19/10)	
Kuossafäbbå	F	DIG	66.442	21.962	0-40	54
					(27/5-31/8)	
Arjelvare	G	DT	66.456	21.957	0-40	42
					(1/6-31/8)	

ANA Analog vertical-component station. Teledyne-Geotech Portacorder RV-320B and seismometer S-500. Continuous recording.

DIG Digital 3-component station. Lennartz Encoder 5000 (station B 5800) and Mark seismometer L4A-3D. Trigger mode recording.

DT Digital vertical-component station. Telemetric transmission to station F. Lennartz transmitter 4001 and Mark seismometer L4A. Triggered simultaneously with parent station.

GR Gain-ranging amplifier.

Table 1. Locations and technical data of the stations.

Station	Code	Type	Location		Filter (Hz)	Gain (dB)
			Lat. ($^{\circ}$ N)	Lon ($^{\circ}$ E)		
Brakarberget	A	ANA	66.651	22.368	10-50	78
					(2/6-3/6)	
					5-25	78
					(3/6-5/6)	
					5-25	84
					(5/6-20/8)	
					10-25	90
					(20/8-19/10)	
Nitsån	B	DIG	66.692	22.224	0-40	GR
					(26/5-19/10)	
Kängelberget	C	DIG	66.636	22.112	0-80	48
					(22/5-26/5)	
					0-80	54
					(26/5-8/7)	
					0-80	60
					(8/7-19/10)	
Renberget	D	ANA	66.543	22.075	5-25	72
					(26/5-8/6)	
					10-50	90
					(8/6-19/10)	
Passeberget	E	DIG	66.514	21.854	0-80	60
					(1/6-19/10)	
Kuossafåbbå	F	DIG	66.442	21.962	0-40	54
					(27/5-31/8)	
Arjelvare	G	DT	66.456	21.957	0-40	42
					(1/6-31/8)	

ANA Analog vertical-component station. Teledyne-Geotech Portacorder RV-320B and seismometer S-500. Continuous recording.

DIG Digital 3-component station. Lennartz Encoder 5000 (station B 5800) and Mark seismometer L4A-3D. Trigger mode recording.

DT Digital vertical-component station. Telemetric transmission to station F. Lennartz transmitter 4001 and Mark seismometer L4A. Triggered simultaneously with parent station.

GR Gain-ranging amplifier.

VELOCITY MODEL

Four test explosions, each of 5 kg dynamite, were carried out in the area (Fig. 1). Pg-waves were excellently recorded with sharp onsets, whereas Sg-waves were not. Only in one case was a clear S onset observed. No exact shot times were recorded. Thus, there is some uncertainty in the obtained, simple constant-velocity model, $P_g = 5.82$ km/s and $S_g = 3.36$ km/s. Also alternative models have been attempted in the localization procedure, and rather drastic changes (10%) are shown not to move the epicentres by more than a few km, at most.

DATA REDUCTION

Data processing of the digital data was done with Lennartz Decoder 5000/5800 - cf. Table 1 - and Hewlett-Packard computer HP-1000. From the trigger lists, several thousand "events" had to be examined. After various automatic and manual steps, at which false triggers, teleseismic events, and regional events at distances larger than 40 km, including hundreds of mine explosions in Swedish Lapland, were eliminated, the number of near-located earthquakes had narrowed into about 20.

EVENT LOCATION

The location program HYPOINV1 (Klein, 1978) has been used for nine near earthquakes, from each of which the set of digital-data onsets is sufficient to provide a solution. The precision of arrival times is about 0.001 s from this kind of data; it is almost 2 orders lower from analog records. In these nine cases, three or more digital stations have readable Pg or Sg onsets, and at least one of the stations has both Pg and Sg. Two solutions give stable focal depths, 8 and 9 km, respectively. The obtained locations are plotted in Figures 3 and 4, and also given in Table 2.

For each of two additional events (no. 10 and 11 in Table 2), digital data provide two possible locations. Whereas no distinction between the

solutions can be obtained for event no. 10, the Pg and Sg onsets at the analog station D (Renberget) are sufficiently clear to favour one solution for event no. 11. The two possible locations for event no. 10 and the one for event no. 11 are shown in Fig. 3.

Table 2. Located Earthquakes

Event	Date	Origin time	Location	
	y m d	h m s (GMT)	Lat. ($^{\circ}$ N)	Lon. ($^{\circ}$ E)
1	870527	11 55 56	66.609	22.419
2	870623	20 52 14	66.393	22.032
3	870623	22 26 42	66.392	22.029
4	870627	15 42 06	66.376	21.753
5	870627	21 04 59	66.501	22.143
6	870718	04 02 32	66.505	21.234
7	870724	17 22 41	66.392	22.071
8	870905	09 15 21	66.512	22.162
9	871015	02 27 40	66.426	22.129
10*	870717	11 36 51	66.688	21.971
10*			66.593	22.293
11**	870822	07 38 53	66.406	22.111

* Two indistinguishable solutions (see Fig. 3).

** One of two possible digital-data solutions selected on basis of analog-record times (Renberget).

As mentioned above, the precision of onset times on analog records is not very high, and especially Sg-phases are hard to pick. The analog stations were operated with the main purpose to quickly and easily identify local events. Fig. 5 displays records from one analog and one digital station for one of the near earthquakes (no. 7).

FOCAL MECHANISMS

In spite of the small distance to many events, the number and azimuthal coverage of employed stations are insufficient to provide good fault-plane solutions. A modified version of the computer program FOCMEC (Snook et al., 1984) has been applied to derive focal mechanisms for earthquakes with four or more Pg-wave polarities or Sg/Pg-wave amplitude ratios (six of the nine events). An algorithm described by Wahlström

(1987) for selection and processing of the data has been followed. Although we have been cautious to read amplitudes from the first period of the respective phase, amplitude data are less reliable than polarities in mechanism studies, also at these very small distances. For the events 2, 3 and 7, which are located close to one another (Fig. 3), a composite-mechanism solution has been performed using exclusively the polarity data. In the APPENDIX we show plots of possible mechanisms. Apparently, many mechanisms are poorly restrained. A feature of most mechanisms of earthquakes in intraplate areas on both sides of the North Atlantic (and elsewhere) is the predominance of the horizontal component of the deviatoric compressional stress (P axis in the APPENDIX), reflecting the "pushing" force at the Mid-Atlantic Ridge (see, e.g., Richardson et al., 1979). That this characteristic is not observed in many of our solutions does probably not so much indicate deviating tectonophysical behaviour, but rather reflects the poor input data.

DYNAMIC PARAMETERS OF THE SOURCE

Sg-signals recorded by digital 3-component seismographs were converted to radial and transverse components. The ground-amplitude spectrum of the larger-amplitude transverse component was then computed. The low-frequency level and the corner frequency were measured from each spectrum which has the expected simple shape (Fig. 6). As an example, Fig. 6 shows the various steps of this process for event no. 2 recorded at station E (Passeberget).

Based on the spectral level and the corner frequency, the seismic moment, radius of focal area, average relative displacement and stress drop are computed, under the assumption of Brune's (1970, 1971) circular-fault model. Spherical spreading is assumed at these small distances. Table 3 shows the resulting values. Corner frequencies range from 12 to 30 Hz and the spectral low-frequency level from 8×10^{-5} to 6×10^{-3} $\mu\text{m-s}$. Fault radii are 40 - 100 m, displacements 0.07 - 8 mm, and stress drops 0.05 - 7 MPa.

Table 3. Dynamic source parameters.

Event	Seismic moment (Nm)	Magnitude M_L (UPP)	Fault radius (km)	Displacement (mm)	Stress drop (MPa)
1	0.3×10^{12}	1.5	0.1	0.3	0.1
2	0.8×10^{11}	0.9	0.07	0.2	0.2
3	0.5×10^{11}	0.7	0.07	0.1	0.05
4	0.1×10^{12}	1.0	0.08	0.2	0.09
5	0.2×10^{11}	0.3	0.06	0.07	0.05
6	0.1×10^{13}	2.0	0.04	8	7
7	0.2×10^{12}	1.3	0.06	0.7	0.4
8	0.5×10^{12}	1.7	0.08	0.8	0.5
9	0.2×10^{12}	1.3	0.07	0.4	0.3

Seismic moments are 5×10^{10} to 1×10^{12} Nm, and the magnitudes, M_L (UPP), estimated from the relation between moment and magnitude proposed by Slunga (1982), accordingly range from 0.7 to 2.0. A confirmation on the order of computed magnitudes is that the largest event, no. 6, was recorded at the permanent-network station in Kiruna with a magnitude of 1.9.

DISCUSSION AND RECOMMENDATIONS

For the first time in Sweden a close-in seismic network has been operating during a time period of several months. Near earthquakes, distance < 40 km, have been recorded with a frequency of about one per week. This is concordant with the activity recorded during a preparatory study in the same region in 1983 (Wahlström and Kulhanek, 1983). The magnitude is 2 or smaller (M_L (UPP)), and at this moment it is hard to tell if this represents a normal microseismicity rate in the Baltic Shield or if it indicates an enhanced activity in this region. Almost all located events occurred on the eastern side of the postglacial fault segments. Several show good agreement with "major" faults extended

roughly perpendicular to the segments. The major faults possibly reach to the bottom of the lithosphere (H. Henkel, personal communication). The concentration of events to smaller regions is interesting and should be considered in the selection of future station sites. Two earthquakes have well-defined focal depths of 8 and 9 km, respectively. However, derived possible fault-plane orientations are too poorly restrained to shed further light on the tectonophysical connection between faults and earthquakes.

For a future investigation, the following recommendations for improvement are given:

- Increased number of digital stations.

Effects: -More detected events.
 -Improved velocity model.
 -More and better located earthquakes.
 -More and better fault-plane solutions.
 -More complete and reliable seismotectonic description and interpretation.

- More and stronger test explosions.

Effects: -Improved velocity model.

- Better reliability of station operation.

Effects: -More detected earthquakes.
 -More data to process.

- Software development.

Effects: -Improved and more rapid data reduction and analysis (this will to some part be achieved also from the previous year's experience).

Acknowledgements

Ota Kulhanek provided support and suggestions during the work and has reviewed the text. The local residents Mr. Holger Nordmark and Mr. Per-

Arne Jönsson assisted in the field work. Fig. 4 was processed with the EBBA graphic system at the Geological Survey of Sweden, thanks to Herbert Henkel.

REFERENCES

- Brune, J.N. (1970). Tectonic stress and the spectra of seismic shear waves from earthquakes. *J. Geophys. Res.* 75, 4997-5009.
- Brune, J.N. (1971). Correction to tectonic stress and the spectra of seismic shear waves from earthquakes. *J. Geophys. Res.* 76, 5002.
- Henkel, H. (1987). Tectonic studies in the Lansjärv region. Svensk Kärnbränslehantering AB, Technical Report, in press.
- Klein, F.W. (1978). Hypocenter location program: HYPONVERSE, Part 1: User's guide. Open-file report 78-694, U.S. Geological Survey, Menlo Park, Calif.
- Richardson, R.M., Solomon, S.C., and Sleep, N.H. (1979). Tectonic stress in the plates. *Rev. Geophys. Space Phys.* 17, 981-1019.
- Slunga, R. (1982). Research on Swedish earthquakes 1980-1981. FOA Report C 20477-T1, 189 pp.
- Snoke, J.A., Munsey, J.W., Teague, A.G., and Bollinger, G.A. (1984). A program for focal mechanism determination by combined use of polarity and SV-P amplitude ratio data. *Earthquake Notes* 55:3, 15.
- Wahlström, R. (1987). Focal mechanisms of earthquakes in southern Quebec, southeastern Ontario, and northeastern New York with implications for regional seismotectonics and stress field characteristics. *Bull. Seismol. Soc. Am.* 77, 891-924.
- Wahlström, R., and Kulhanek, O. (1983). The Lansjärv fault - seismically active or dead? *Geol. Föreningens i Stockholm Förhandlingar* 105, 334.

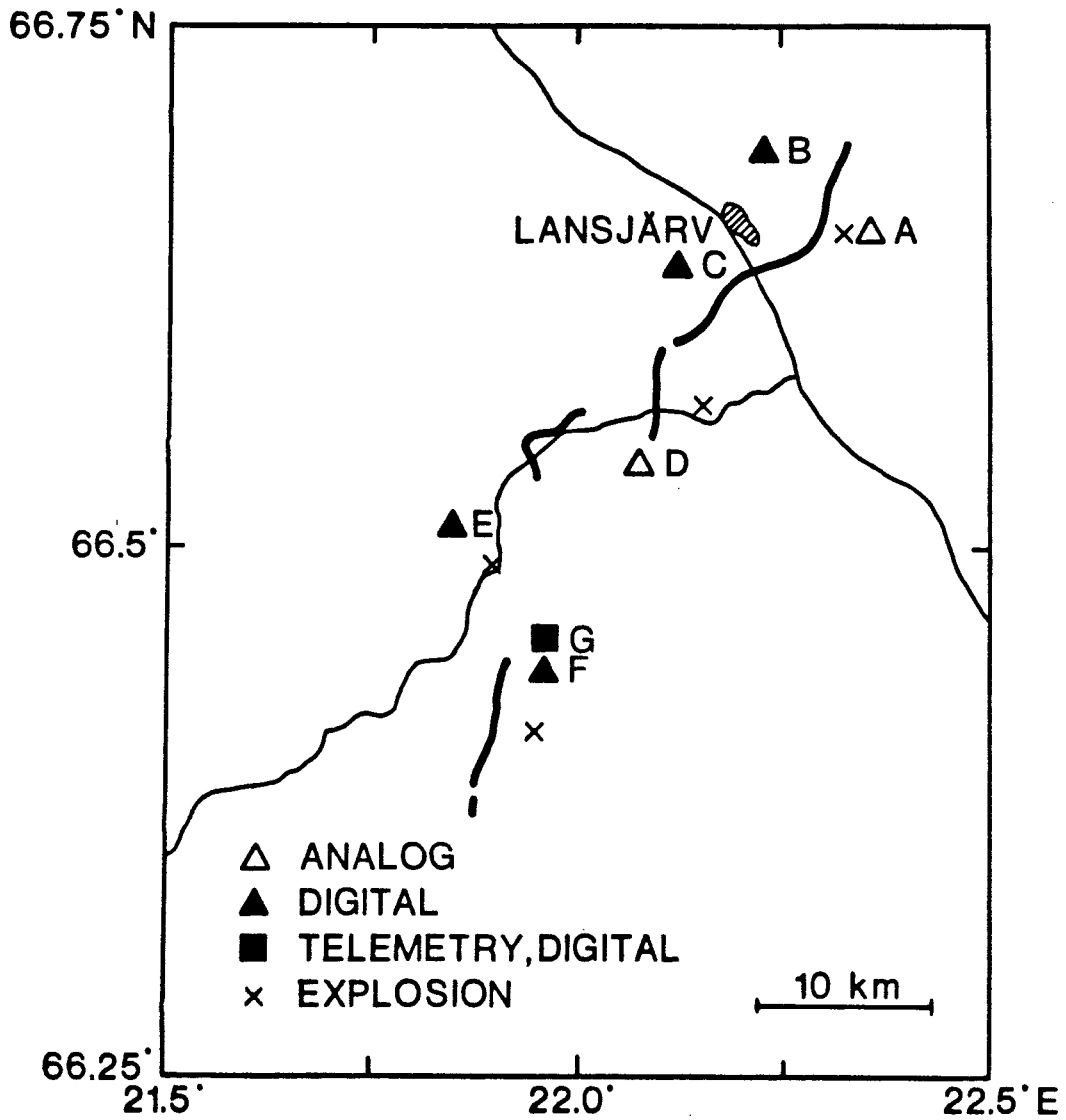


Fig. 1. Locations of fields stations and explosion sites. Thick lines show the Lansjärv post-glacial fault segments, thin lines main roads.

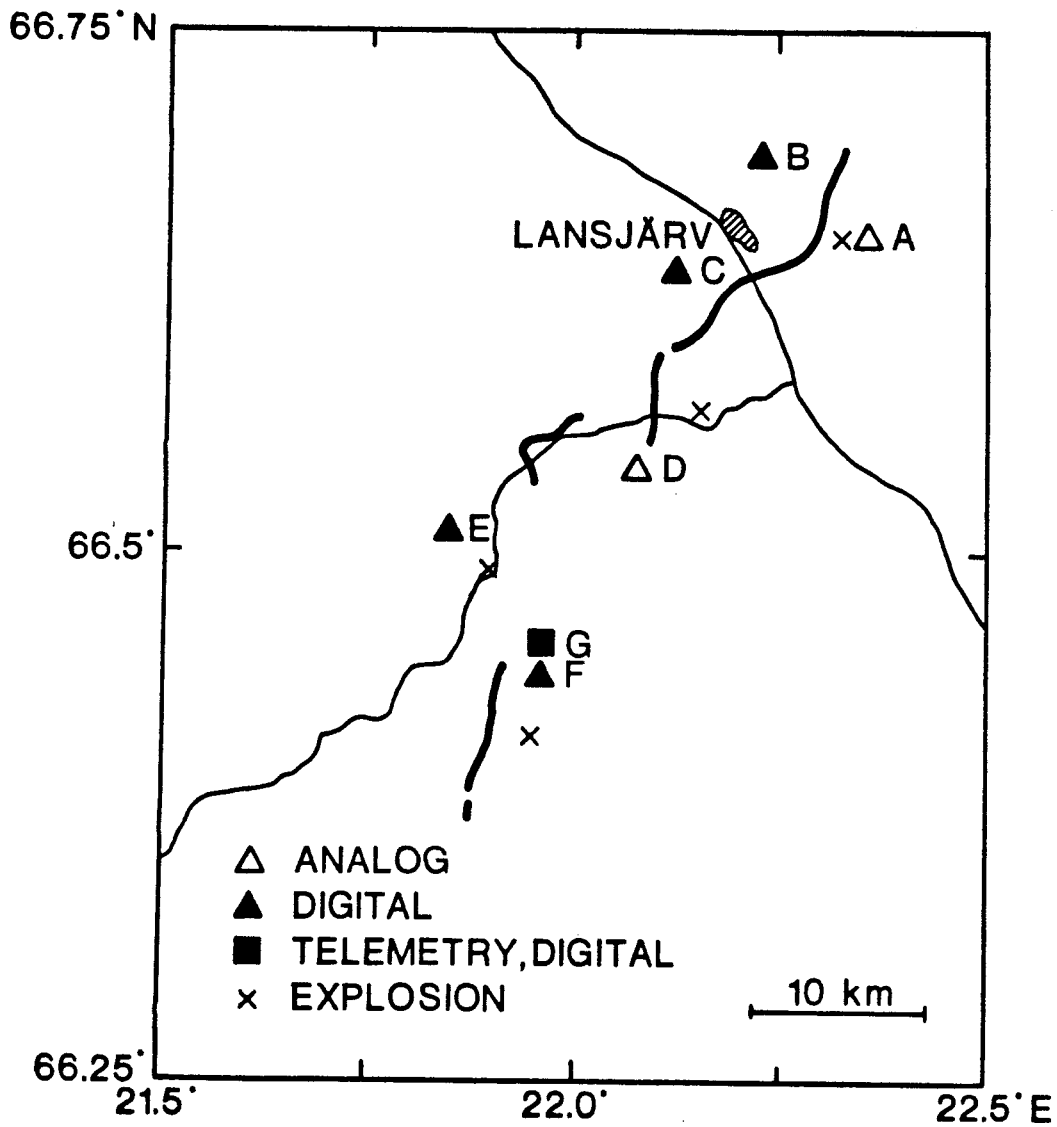


Fig. 1. Locations of fields stations and explosion sites. Thick lines show the Lansjärv post-glacial fault segments, thin lines main roads.

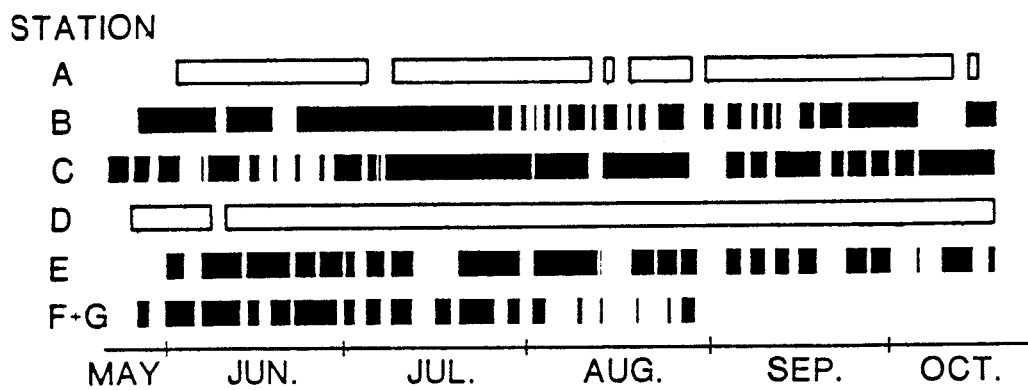


Fig. 2. Times of operation of the seven stations. Open bars denote analog stations, filled bars digital stations (cf. Table 1 and Fig. 1). Station G started to transmit telemetric signals to station F on June 1.

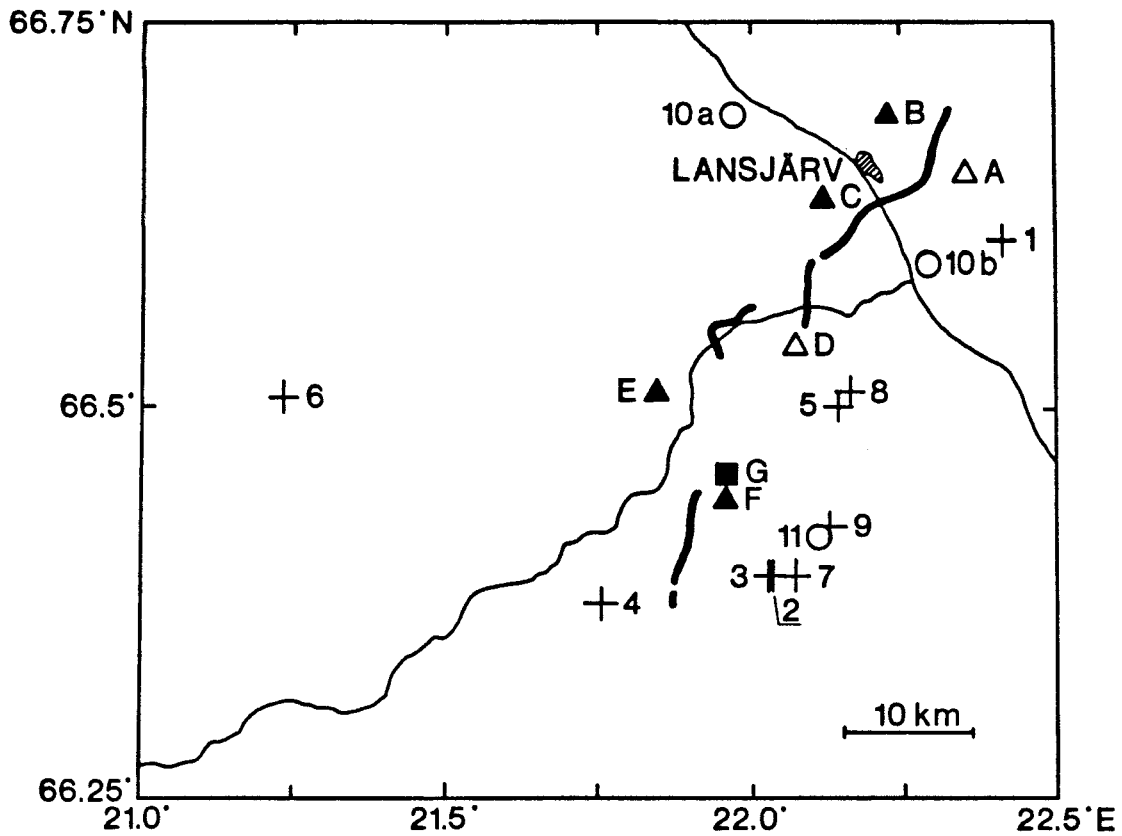


Fig. 3. Locations of 11 earthquakes (Table 2). Events 1-9 (+) are located from three or more digital stations; events 10 and 11 (O) from two digital stations, thus providing two possible solutions each. For event 11, one of the solutions has been selected from supplementary analog-station data. Other notation as in Fig. 1.

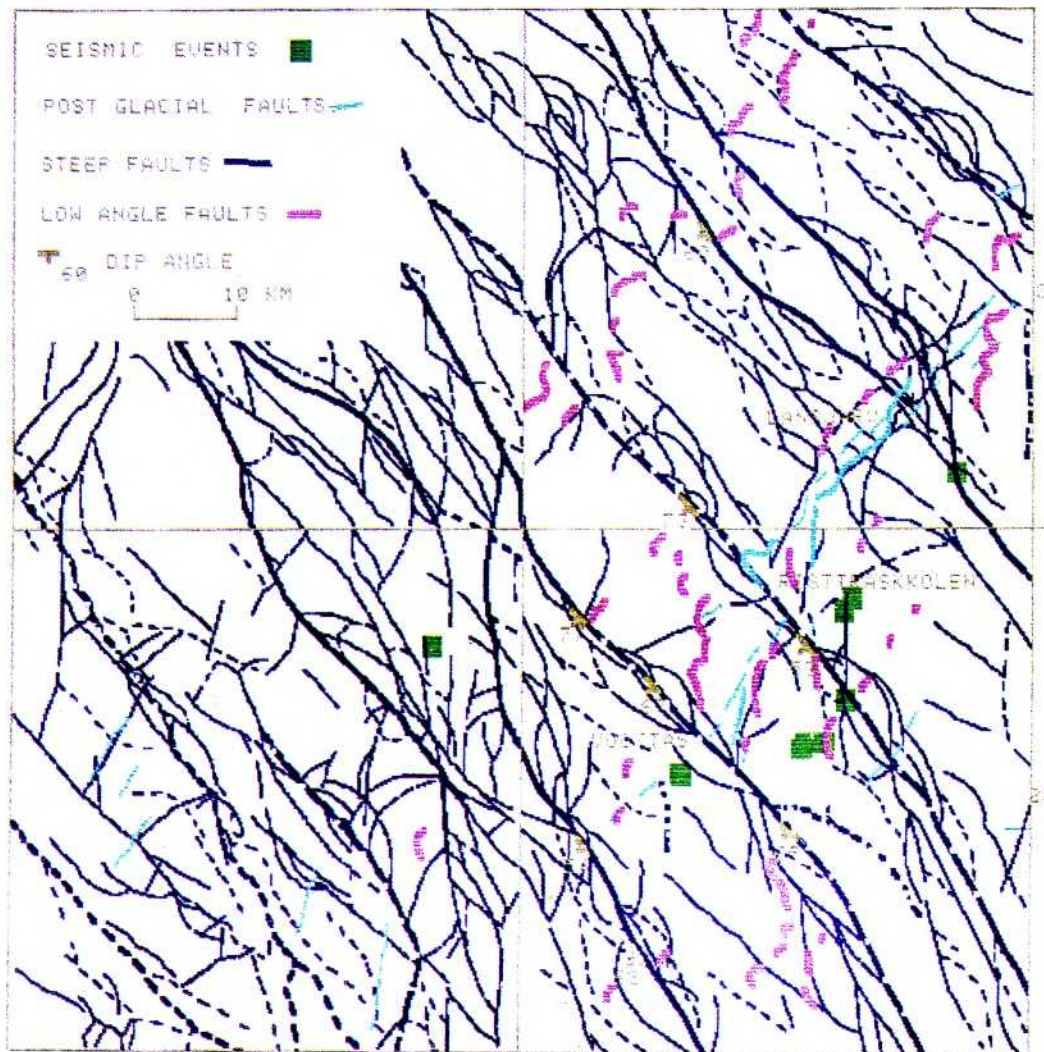


Fig. 4. Epicentres of events 1-9 of Fig. 3 plotted on a tectonic map after Henkel (1987). In six cases, the correlation with southwest dipping major tectonic lineaments is good.

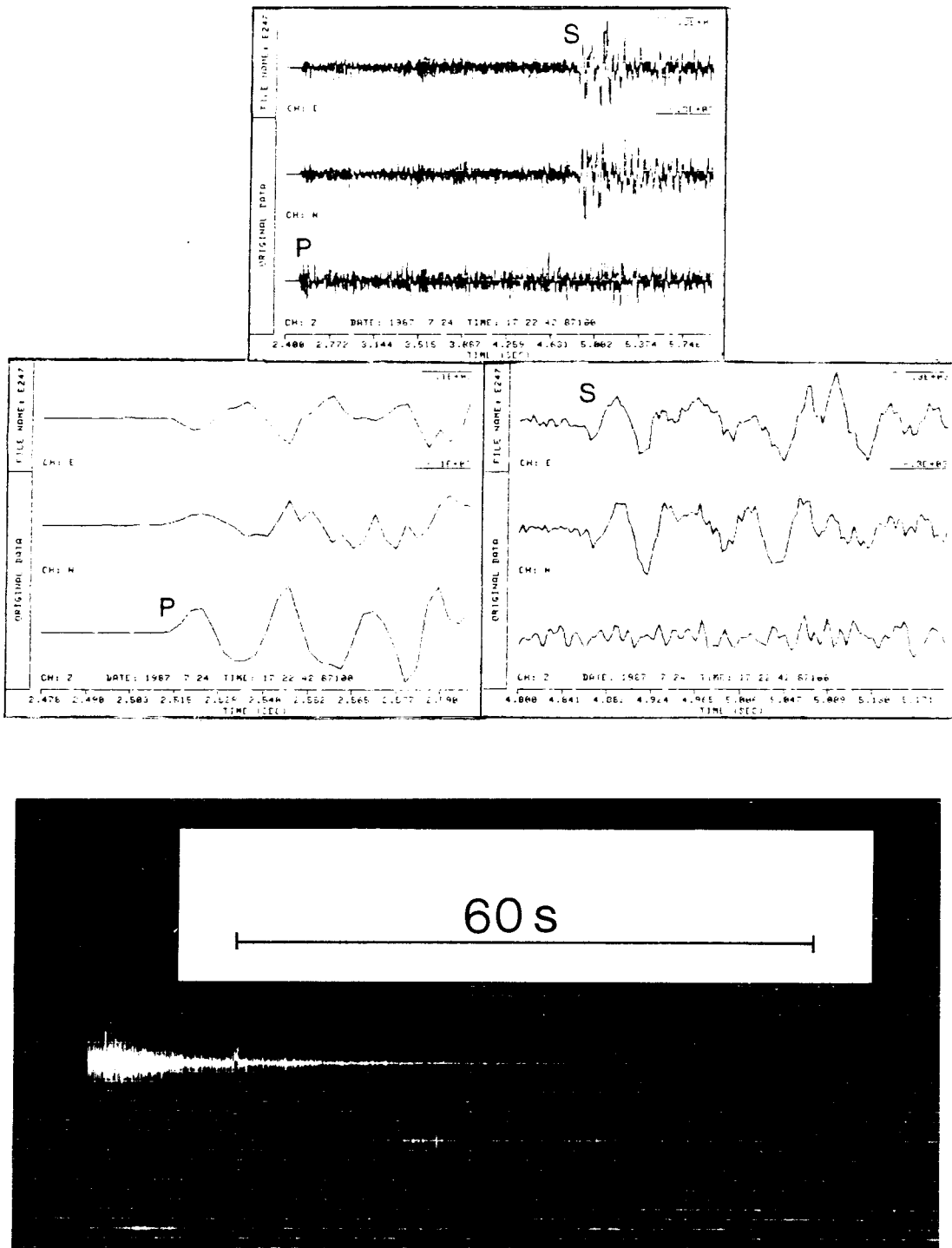


Fig. 5. Records from stations E (Passeberget; digital, top) and D (Renberget; analog, bottom) for the event no. 7 (Table 2). For station E, P and S phases are marked on playouts with different time resolution. The components are, from top to bottom, EW, NS and vertical. A trace motion upward corresponds to ground motion to the W, S and down, respectively.

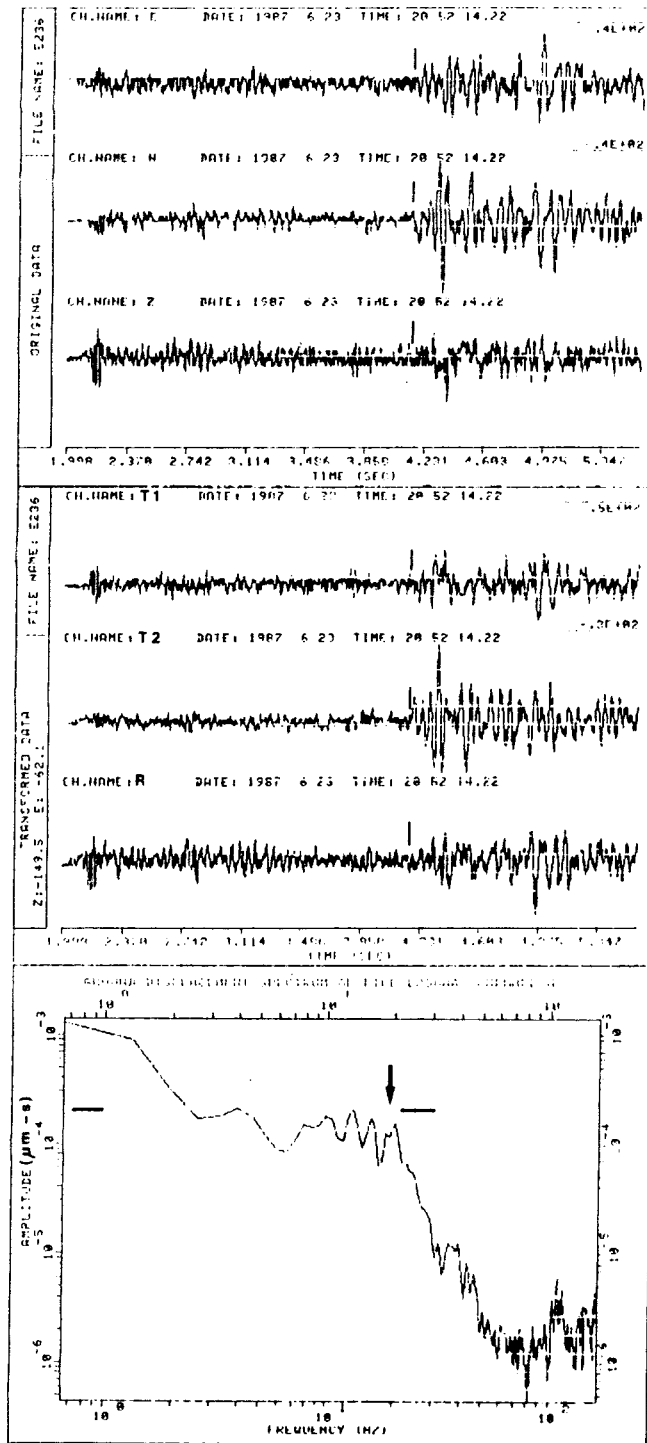
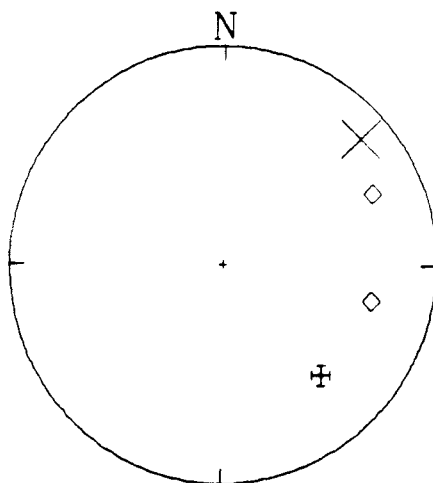


Fig. 6. Records and spectrum of event no. 2 at station E (Passeberget). Top: E, N and Z components. Centre: Transverse (T1, T2) and radial components. Bottom: S-wave amplitude spectrum of T2 component yielding a low-frequency level of $2 \cdot 10^{-4}$ $\mu\text{m-s}$ and a corner frequency of 19 Hz.

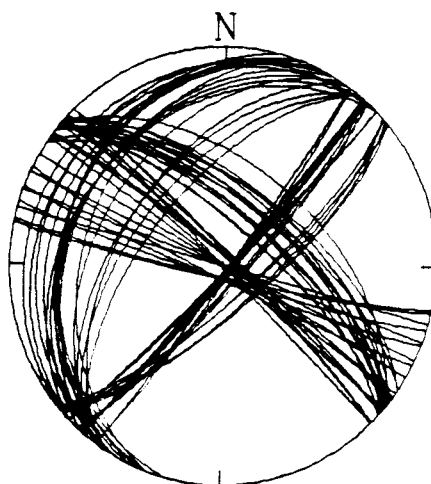
APPENDIX

Input data and sets of focal-mechanism solutions. Each page shows lower-hemisphere projection plots of the focal sphere, displaying, from top to bottom, the input data, the set of accepted pairs of nodal planes, and the set of accepted stress axes and null vectors. For the events 2, 4 and 5, no solutions have been attempted due to sparse data. The last page shows the composite-mechanism solution for events 2, 3 and 7 based only on polarity data.

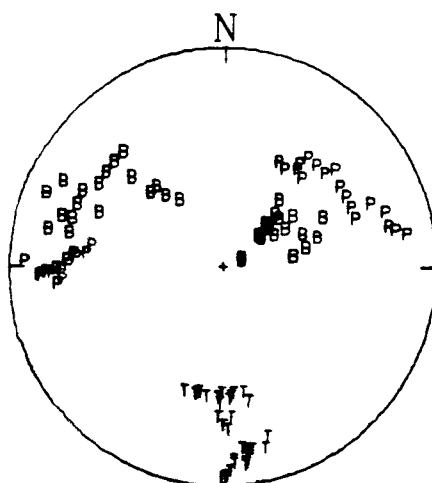
Input data: \oplus impulsive compression (weight 1)
 \diamond impulsive dilatation (weight 1)
 - emergent dilatation (weight 1/2)
 X $\log(\text{ampl}(\text{SV})/\text{ampl}(\text{P}))$ (size of symbol increases with increasing amplitude ratio).
Output data: P compressive-stress axis
 T tensile-stress axis
 B null vector.



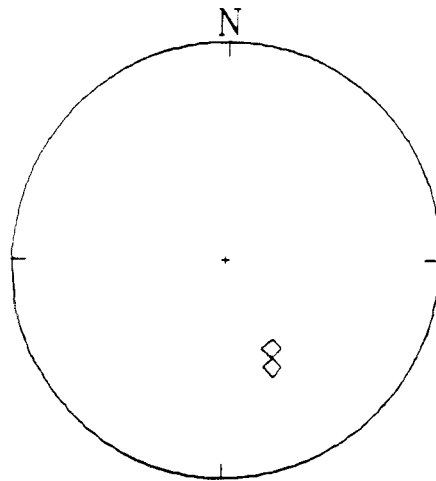
27-5-87 11:56



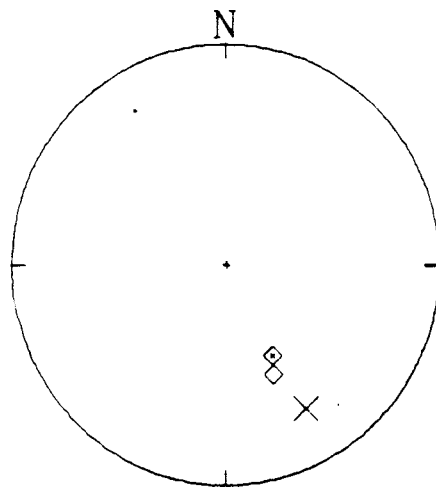
27-5-87 11:56



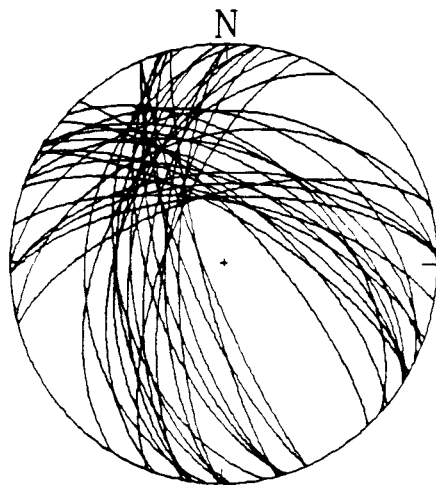
27-5-87 11:56



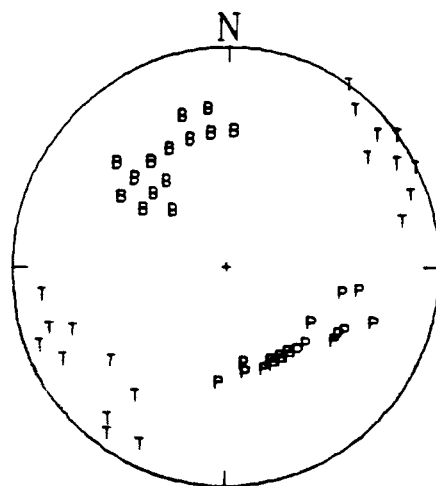
23-6-87 20:52



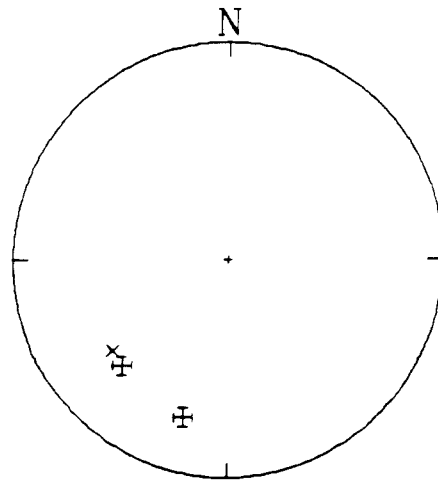
23-6-87 22:26



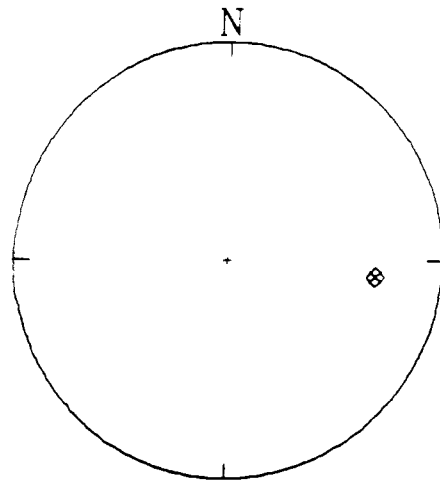
23-6-87 22:26



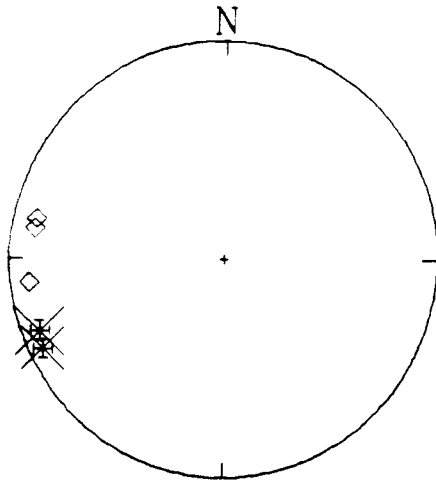
23-6-87 22:26



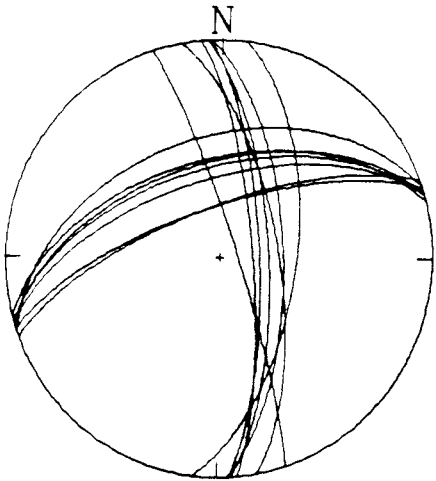
27-6-87 15:42



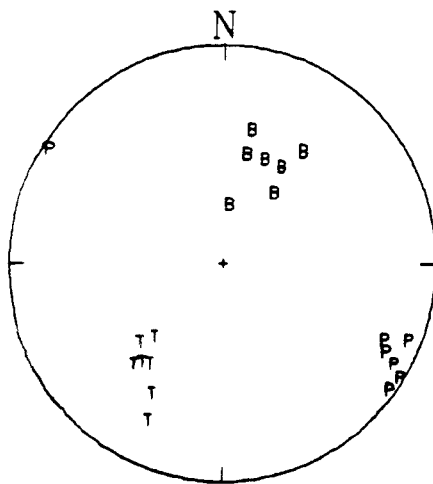
27-6-87 21:05



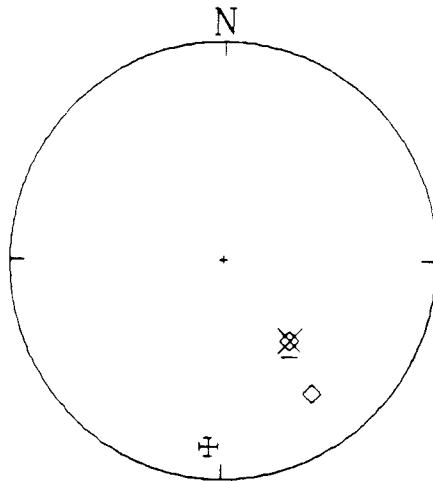
18-7-87 04:02



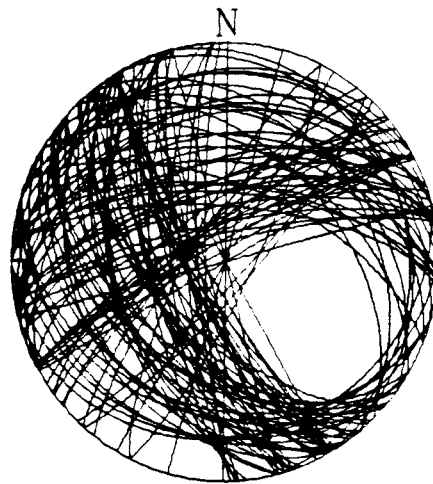
18-7-87 04:02



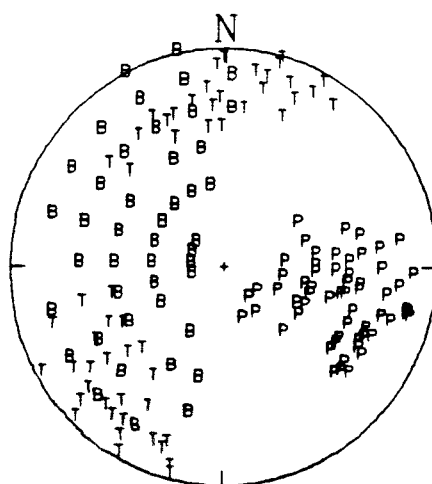
18-7-87 04:02



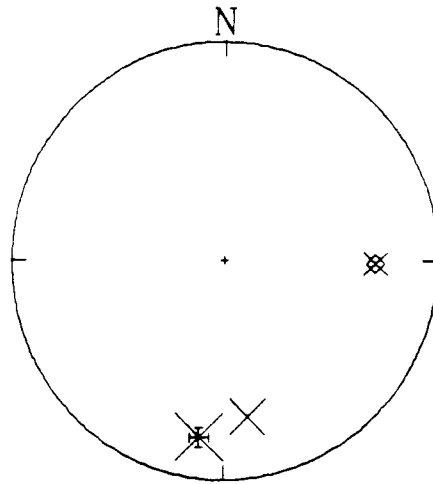
24-7-87 17:22



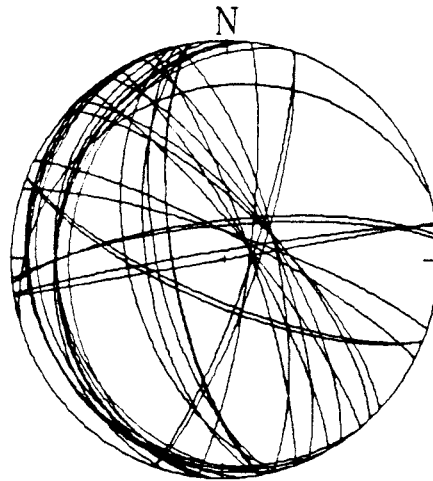
24-7-87 17:22



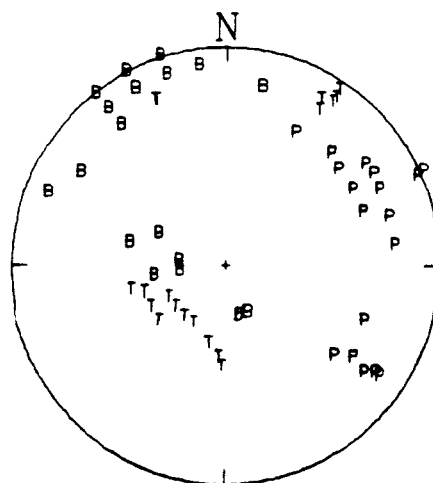
24-7-87 17:22



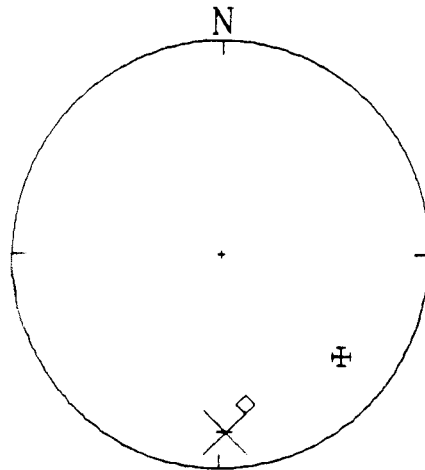
5-9-87 09:15



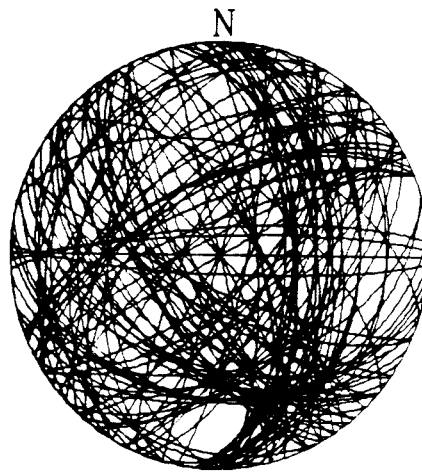
5-9-87 09:15



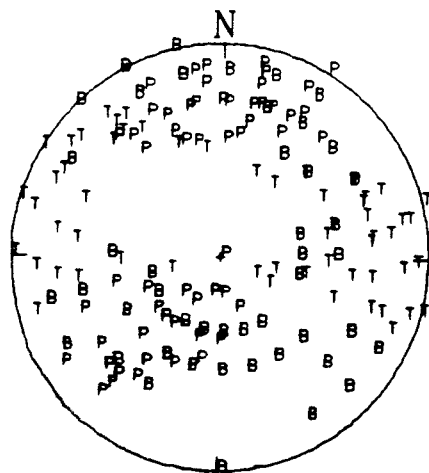
5-9-87 09:15



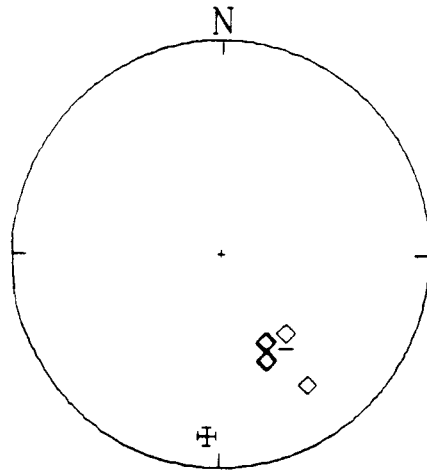
15-10-87 02:27



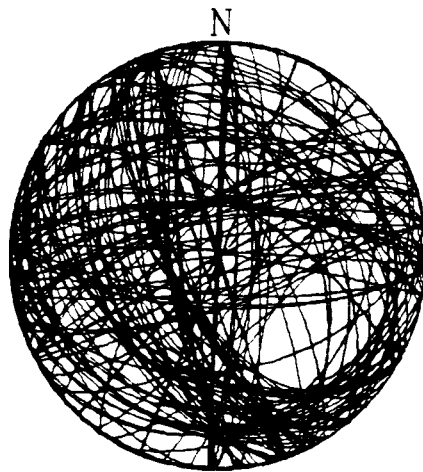
15-10-87 02:27



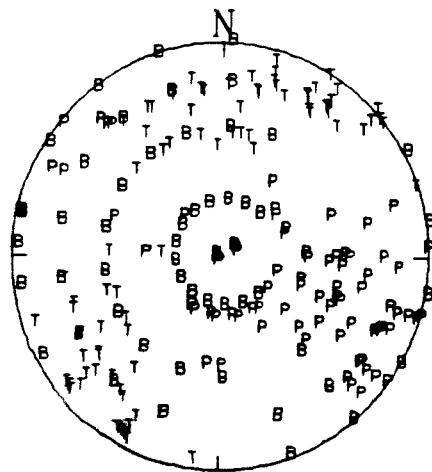
15-10-87 02:27



EVENTS 2, 3 & 7 COMP.



EVENTS 2, 3 & 7 COMP.



EVENTS 2, 3 & 7 COMP.

List of SKB reports

Annual Reports

1977-78

TR 121

KBS Technical Reports 1 – 120.

Summaries. Stockholm, May 1979.

1979

TR 79-28

The KBS Annual Report 1979.

KBS Technical Reports 79-01 – 79-27.

Summaries. Stockholm, March 1980.

1980

TR 80-26

The KBS Annual Report 1980.

KBS Technical Reports 80-01 – 80-25.

Summaries. Stockholm, March 1981.

1981

TR 81-17

The KBS Annual Report 1981.

KBS Technical Reports 81-01 – 81-16.

Summaries. Stockholm, April 1982.

1982

TR 82-28

The KBS Annual Report 1982.

KBS Technical Reports 82-01 – 82-27.

Summaries. Stockholm, July 1983.

1983

TR 83-77

The KBS Annual Report 1983.

KBS Technical Reports 83-01 – 83-76

Summaries. Stockholm, June 1984.

1984

TR 85-01

Annual Research and Development Report 1984

Including Summaries of Technical Reports Issued during 1984. (Technical Reports 84-01–84-19) Stockholm June 1985.

1985

TR 85-20

Annual Research and Development Report 1985

Including Summaries of Technical Reports Issued during 1985. (Technical Reports 85-01-85-19) Stockholm May 1986.

1986

TR 86-31

SKB Annual Report 1986

Including Summaries of Technical Reports Issued during 1986 Stockholm, May 1987

1987

TR 87-33

SKB Annual Report 1987

Including Summaries of Technical Reports Issued during 1987 Stockholm, May 1988

Technical Reports

1988

TR 88-01

Preliminary investigations of deep ground water microbiology in Swedish granitic rocks

Karsten Pedersen

University of Göteborg

December 1987

TR 88-02

Migration of the fission products strontium, technetium, iodine, cesium and the actinides neptunium, plutonium, americium in granitic rock

Thomas Ittner¹, Börje Torstenfelt¹, Bert Allard²

¹Chalmers University of Technology

²University of Linköping

January 1988

TR 88-03

Flow and solute transport in a single fracture. A two-dimensional statistical model

Luis Moreno¹, Yvonne Tsang², Chin Fu Tsang², Ivars Neretnieks¹

¹Royal Institute of Technology, Stockholm, Sweden

²Lawrence Berkeley Laboratory, Berkeley, CA, USA

January 1988

TR 88-04

Ion binding by humic and fulvic acids: A computational procedure based on functional site heterogeneity and the physical chemistry of polyelectrolyte solutions

J A Marinsky, M M Reddy, J Ephraim, A Mathuthu

US Geological Survey, Lakewood, CA, USA

Linköping University, Linköping

State University of New York at Buffalo, Buffalo, NY, USA

April 1987

TR 88-05

Description of geophysical data on the SKB database GEOTAB

Stefan Sehlstedt

Swedish Geological Co, Luleå

February 1988

TR 88-06

Description of geological data in SKBs data-base GEOTAB

Tomas Stark
Swedish Geological Co, Luleå
April 1988

TR 88-07

Tectonic studies in the Lansjärv region

Herbert Henkel
Swedish Geological Survey, Uppsala
October 1987

TR 88-08

**Diffusion in the matrix of granitic rock.
Field test in the Stripa mine. Final report.**

Lars Birgersson, Ivars Neretnieks
Royal Institute of Technology, Stockholm
April 1988

TR 88-09

The kinetics of pitting corrosion of carbon steel. Progress report to June 1987

G P Marsh, K J Taylor, Z Sooi
Materials Development Division
Harwell Laboratory
February 1988

TR 88-10

**GWHRT – A flow model for coupled groundwater and heat flow
Version 1.0**

Roger Thunvik¹, Carol Braester²
¹ Royal Institute of Technology, Stockholm
² Israel Institute of Technology, Haifa
April 1988

TR 88-11

**Groundwater numerical modelling of the Fjällveden study site – Evaluation of parameter variations
A hydrocoin study – Level 3, case 5A**

Nils-Åke Larsson¹, Anders Markström²
¹ Swedish Geological Company, Uppsala
² Kemakta Consultants Co, Stockholm
October 1987